The retinoblastoma gene pathway regulates the postmitotic state of hair cells of the mouse inner ear

Johanna Mantela[1], Zhe Jiang[2], Jukka Ylikoski[1], Bernd Fritzsch[3], Eldad Zacksenhaus[2] and Ulla Pirvola[1,*]

[1]Institute of Biotechnology, University of Helsinki, 00014 Helsinki, Finland
[2]Departments of Medicine, Laboratory Medicine and Pathobiology and Medical Biophysics, Division of Cell and Molecular Biology, Toronto General Research Institute, University Health Network, University of Toronto, Toronto, Ontario M5G-2M1, Canada
[3]Creighton University, Department of Biomedical Sciences, Omaha, NE 68178, USA
*Author for correspondence (e-mail: ulla.pirvola@helsinki.fi)

Summary

Precursors of cochlear and vestibular hair cells of the inner ear exit the cell cycle at midgestation. Hair cells are mitotically quiescent during late-embryonic differentiation stages and postnatally. We show here that the retinoblastoma gene *Rb* and the encoded protein pRb are expressed in differentiating and mature hair cells. In addition to *Rb*, the cyclin dependent kinase inhibitor (CKI) *p21* is expressed in developing hair cells, suggesting that p21 is an upstream effector of pRb activity. p21 apparently cooperates with other CKIs, as *p21*-null mice exhibited an unaltered inner ear phenotype. By contrast, *Rb* inactivation led to aberrant hair cell proliferation, as analysed at birth in a loss-of-function/transgenic mouse model. Supernumerary hair cells expressed various cell type-specific differentiation markers, including components of stereocilia. The extent of alterations in stereociliary bundle morphology ranged from near-normal to severe disorganization. Apoptosis contributed to the mutant phenotype, but did not compensate for the production of supernumerary hair cells, resulting in hyperplastic sensory epithelia. The *Rb*-null-mediated proliferation led to a distinct pathological phenotype, including multinucleated and enlarged hair cells, and infiltration of hair cells into the mesenchyme. Our findings demonstrate that the pRb pathway is required for hair cell quiescence and that manipulation of the cell cycle machinery disrupts the coordinated development within the inner ear sensory epithelia.

Key words: Inner ear, Cochlea, Vestibular organ, Hair cell, Proliferation, Differentiation, Apoptosis, Cell cycle, Mitosis, Polyploidy, *Rb* (*Rb1*), *p21* (*Cdkn1a*), Mouse

Introduction

The auditory sensory epithelium of the cochlea, the organ of Corti, and the sensory epithelia of vestibular organs are composed of hair cells (HCs) and supporting cells. Inner ear HCs are mechanosensory cells, which convert mechanical force produced by sound waves and head movements into neural impulses. Hair cells and supporting cells have common precursors, as shown in the chick auditory organ (Fekete et al., 1998). In the mouse, these precursors permanently exit the cell cycle in midgestation (Ruben, 1967). In the presumptive organ of Corti, cell cycle exit is followed by the upregulation of the basic helix-loop-helix (bHLH) gene *Math1* (*Atoh1* – Mouse Genome Informatics), which initiates HC differentiation (Bermingham et al., 1999; Chen et al., 2002; Fritzsch et al., 2005). Differentiating and adult HCs are postmitotic and refractory to mitogens, a likely reason being the activity of negative cell cycle regulators.

A recent study by Chen et al. (Chen et al., 2003) showed that targeted disruption of the gene encoding a member of the Ink4 family of CKIs, *p19* (*Cdkn2d* – Mouse Genome Informatics), leads to abnormal DNA synthesis in postnatal cochlear HCs. Bromodeoxyuridine incorporation was shown to occur at a low rate. Aberrant proliferation was accompanied by

apoptosis and resulted in progressive hearing loss. In contrast to postnatal HCs, *p19* inactivation did not affect the antiproliferative state of HCs during late-embryogenesis, although *p19* was reported to be expressed in the embryonic organ of Corti (Chen et al., 2003). These data suggest that additional CKIs compensate for *p19* deficiency in developing cochlear HCs. Cell cycle regulation downstream of CKIs has not been reported in the cochlea. Furthermore, the mechanisms underlying cell cycle arrest of vestibular HCs have not been explored.

A key regulator of the cell cycle is pRb, the protein product of the *Rb* (*Rb1* – Mouse Genome Informatics) tumour suppressor gene (Weinberg, 1995). pRb is the prototypical member of the pocket protein family, which also comprises p107 and p130. Pocket proteins have both unique and overlapping functions in cell cycle control, in regulation of cell differentiation and survival, and in inhibition of oncogenic transformation (Classon and Harlow, 2002). pRb is a nuclear phosphoprotein. It binds members of the E2f transcription factor family during G1 and represses genes required for G1 to S-transition. In response to mitogens, pRb becomes phosphorylated (inactivated) by cyclin/cyclin dependent kinase (CDK) complexes, resulting in the release of bound E2fs, transcriptional de-repression and cell cycle progression.

Mitogenic signals induce the cell cycle machinery at the level of cyclins and CDKs (Murray, 2004). CDK activation is regulated by various mechanisms, a particularly important one being the inhibition by CKIs (Vidal and Koff, 2000). Inhibition of CDK activity by CKIs maintains pRb in a hypophosphorylated (active) state. There are two families of CKIs, the Ink4 family (p15, p16, p18, p19) and the Cip/Kip family (p21, p27, p57).

Analyses of loss-of-function mutant mice have demonstrated the essential role of *Rb* as a repressor of cell cycle progression during embryogenesis. *Rb* knockouts die in midgestation, between embryonic day 13 (E13) and E14. In addition to ectopic cell cycles, development of the nervous system, skeletal muscles, lens and haematopoietic cells of the mutants is characterized by aberrant differentiation and extensive apoptosis (Clarke et al., 1992; Jacks et al., 1992; Lee et al., 1993; Morgenbesser et al., 1994; Zacksenhaus et al., 1996). Consistently, *Rb* is prominently expressed in these tissues (Jiang et al., 1997). Recent conditional mutagenesis and placental rescue indicate that the apoptotic phenotype of whole-embryo *Rb* knockouts is not caused by cell-autonomous mechanisms in all tissues: apoptosis in the brain largely occurs secondarily to other embryonic defects, whereas apoptosis in skeletal muscles, retina and lens appears to be a direct consequence of *Rb* inactivation (Ferguson et al., 2002; de Bruin et al., 2003; MacPherson et al., 2003; MacPherson et al., 2004; Wu et al., 2003; Chen et al., 2004; Zhang et al., 2004).

How *Rb* regulates cell differentiation is in general poorly understood. The role of *Rb* in differentiation appears to be more versatile than merely indirectly stimulating this process through the inhibition of cell cycle progression. In some cases, it has been possible to separate the effects of *Rb* on cell proliferation and differentiation (Sellers et al., 1998; Liu and Zacksenhaus, 2000; Takahashi et al., 2003; Zhang et al., 2004). In skeletal muscles, *Rb* transcriptionally upregulates genes involved in the late stages of differentiation through the bHLH gene myogenin (Gu et al., 1993; Novitch et al., 1996; Novitch et al., 1999). Similarly, adipocyte differentiation is induced by the positive effect of *Rb* on the transcriptional activity of CCAAT/enhancer-binding proteins (Chen et al., 1996).

We show here that pRb is expressed in inner ear HCs. The lethality of *Rb* knockouts at the stage when part of HCs have not yet started to differentiate precludes the use of these mutants in our studies. To genetically dissect the *Rb* pathway and unravel the requirement for pRb during HC development, we have analysed the inner ear sensory epithelia of *mgRb:Rb*$^{-/-}$ mutants, which are rescued to birth by a hypomorphic *Rb* transgene (Zacksenhaus et al., 1996). The transgene is expressed in the nervous system, but not in non-neuronal tissues (Jiang et al., 2001), including the inner ear HCs (this study). Our results suggest that pRb regulates HC quiescence and that, during development, p21 may act co-operatively with other CKI(s) as an upstream effector of pRb activity. *Rb* loss induced aberrant HC proliferation, but these cells also showed pathological features, including mitotic abnormalities and signs of apoptosis.

Materials and methods

Mice

The NMRI mouse strain was used for the analysis of pRb protein and *Rb* and *p21* mRNA expression in the inner ear. Timed pregnancies were established by the detection of vaginal plug, taken the morning of plug observation as E0.5. Generation and genotyping of *mgRb:Rb*$^{-/-}$ mutant mice have been described previously (Zacksenhaus et al., 1996). *p21*$^{-/-}$ mice were obtained from Jackson Laboratory, originally described by Brugarolas et al. (Brugarolas et al., 1995). *E2f1*$^{-/-}$ and apoptosis protease-activating factor 1 (*Apaf1*)$^{-/-}$ mice have been described previously (Field et al., 1996; Yoshida et al., 1998). Their genotyping and generation of compound *mgRb:Rb*$^{-/-}$:*E2f1*$^{-/-}$ and *mgRb:Rb*$^{-/-}$:*Apaf1*$^{-/-}$ mutants have been described previously (Jiang et al., 2000; Guo et al., 2001).

Histology, immunohistochemistry and TUNEL staining

Whole heads of E12.5, E13.5, E14.5, E15.5 and E16.5 embryos, and dissected inner ears of E17.5 and E18.5 embryos and of postnatal day (PN) 2 and 6 pups were fixed overnight in 4% paraformaldehyde (PFA), embedded in paraffin and cut to 5-μm sections. Inner ears of 8-week-old mice were perilymphatically fixed with PFA, immersed in this fixative overnight, decalcified with 0.5 M EDTA and embedded in paraffin wax. Following antibodies were used: monoclonal Rb (BD Biosciences), polyclonal myosins VI and VIIa (Hasson et al., 1997; Pirvola et al., 2004), monoclonal calretinin and calbindin (Swant), polyclonal phospho-histone H3 (Ser10, Cell Signaling Technology) (Pirvola et al., 2004), polyclonal espin (Zheng et al., 2000), polyclonal p75 neurotrophin receptor (p75NTR) (Pirvola et al., 2002), monoclonal p27 (Neomarkers), and monoclonal (rabbit) cleaved caspase 3 (Cell Signaling Technology). Detection was carried out with the Vectastain Elite ABC kit or the Vectastain Mouse-On-Mouse kit and the diaminobenzidine substrate (Vector Laboratories). Methyl Green was used for counterstaining. For double-labelling experiments, PFA-fixed inner ears of E18.5 embryos were cryosectioned, and phospho-histone H3 and calretinin or calbindin were used as primary antibodies. Binding was visualized by fluorochrome-conjugated secondary antibodies (Alexa Fluor 488 and 568, Molecular Probes). In addition to cleaved caspase 3 immunostaining, TUNEL method-based Fluorescein In Situ Cell Death Detection Kit (Roche) was used to detect apoptotic cells.

Semi-thin sections

Inner ears of *mgRb:Rb*$^{-/-}$ mice and control littermates were dissected at E18.5 and fixed overnight in 2.5% glutaraldehyde, postfixed in 1% osmium tetroxide and embedded in Epon. Sections (0.5 μm) were cut in transverse (midmodiolar) plane and stained with 2% Toluidine Blue.

In situ hybridization

In situ hybridization was performed with ^{35}S-labelled riboprobes on PFA-fixed paraffin wax sections according to the protocol by Wilkinson and Green (Wilkinson and Green, 1991). *Rb*, *p107* (*Rbl1* – Mouse Genome Informatics), *p130* (*Rbl2* – Mouse Genome Informatics), *p21* (Cdkn1a – Mouse Genome Informatics), *Math1*, fibroblast growth factor 8 (*Fgf8*), *Fgf10*, *Brn3c* (*Pou4f3* – Mouse Genome Informatics) and brain-derived neurotrophic factor (*Bdnf*) cDNAs were used.

Results

pRb expression in the inner ear sensory epithelia

We first studied pRb expression in normal inner ears by immunohistochemistry (Fig. 1A-H). We confirmed at all stages that pRb expression pattern corresponded to that of *Rb* mRNA, as analysed by in situ hybridization. Weak and diffuse pRb expression was initially, at E12.5, detected in the presumptive vestibular sensory patches. The expression was upregulated in the early-differentiating vestibular HCs at E13.5 (Fig. 1A). In the vestibular sensory epithelia (saccular and utricular

Fig. 1. pRb expression in hair cells of the inner ear. pRb immunostaining; *Rb* in situ hybridization. (A,B) pRb staining in the early- and later-differentiating HCs of the embryonic saccule. (C,D) pRb and *Rb* expressions in HCs of the late-embryonic utricle. (E) A subpopulation of HCs is pRb-positive in the adult utricle. (F,G) pRb expression in inner and outer HCs of the cochlea at birth and early postnatal life. In addition to HCs, the greater epithelial ridge shows weak expression at birth. (H) In the mature organ of Corti, pRb expression is detected only in inner HCs. Supporting cells are negative at all stages. (I,J) pRb is not expressed in the hyperplastic sensory epithelium of utricle and cochlea of *mgRb:Rb$^{-/-}$* mutants at E18.5. Abbreviations: wt, wild type; sac, saccule; ut, utricle; co, cochlea; IHC, inner hair cell; OHCs, outer hair cells; GER, greater epithelial ridge; HCs, hair cells; SCs, supporting cells. Arrows in G,H,J indicate HCs. Scale bar: 70 μm.
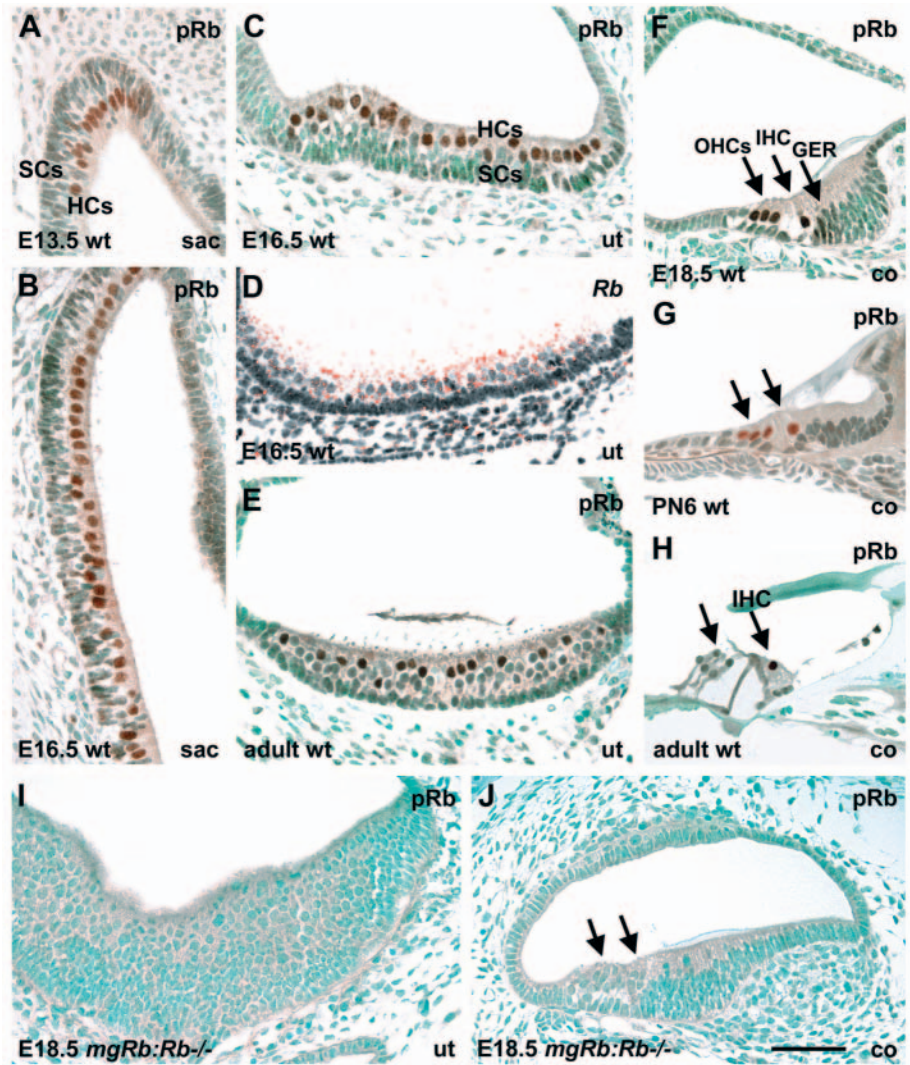
maculae, and ampullary cristae) of late embryonic and early postnatal mice, pRb was detected in the nuclei of the entire HC population (Fig. 1A-D). By contrast, adult vestibular organs showed expression only in a subpopulation of HCs (Fig. 1E). From E12.5 onwards, pRb was weakly expressed in the caudal wall of the cochlear duct, which contains sensory precursor cells (data not shown). In the developing organ of Corti, pRb expression was upregulated at E15.5, at the early stage of morphological differentiation of cochlear HCs. This upregulation was confined to HCs and followed a base-to-apex gradient, corresponding to the differentiation gradient of the auditory organ. Both inner and outer HCs showed pRb-staining during late embryogenesis and early postnatal period (Fig. 1F,G), while during adulthood staining was detected only in inner HCs (Fig. 1H). Supporting cells adjacent to cochlear and vestibular HCs did not show detectable expression (Fig. 1A-H). Importantly, by in situ hybridization, we did not detect expression of the related genes, *p107* and *p130,* in developing HCs (data not shown), suggesting that functional redundancy among pocket proteins is unlikely in these cells.

The dynamic expression of pRb and the lack of detectable levels of *p107* and *p130* in differentiating HCs prompted us to test the in vivo consequences of *Rb* loss in the inner ear. To circumvent midgestational lethality of mice homozygous for a null mutation in *Rb*, we used *mgRb:Rb$^{-/-}$* mice, which are rescued to birth by transgenic expression of a wild-type *Rb* minigene (consisting of a genomic fragment spanning 1.3 kb of the mouse *Rb* promoter plus the first exon and intron fused to exons 2 to 27 of the mouse *Rb* cDNA) (Zacksenhaus et al., 1996). This genetic manipulation leads to suppression of the neurogenic phenotype seen in *Rb* knockouts and reveals a role for pRb in skeletal myogenesis. A severe lens defect and incomplete erythropoiesis have also been noted in these mutant

fetuses (Zacksenhaus et al., 1996; Liu and Zacksenhaus, 2000; Jiang et al., 2000). Consistent with this, the minigene, fused to *lacZ* reporter gene, directs expression exclusively to the nervous system (Jiang et al., 2001). In line with the results obtained in other non-neuronal tissues of *mgRb:Rb$^{-/-}$* embryos, we did not detect *Rb* or pRb expression in their HCs (Fig. 1I,J). Hence, these cells can be viewed as null for *Rb*.

Hyperplasia of the developing auditory sensory epithelium in the absence of *Rb*

Global inner ear morphology of *mgRb:Rb$^{-/-}$* mutants at E17.5 (*n*=8 ears) and E18.5 (*n*=15 ears) was comparable with controls, but distinct differences were seen in the sensory epithelia (Figs 2 and 3). Only minor variations were observed between individual mutants, both at the level of vestibular and auditory sensory epithelia. The normal organ of Corti shows one inner HC and three outer HCs in a midmodiolar, radially sectioned cochlear duct. This was apparent from histology and from the positive staining with myosin VI, a cytoplasmic marker (Fig. 2A). One layer of supporting cells is normally located below HCs on the basilar membrane. The organ of Corti of *mgRb:Rb$^{-/-}$* mutants was hyperplastic because of excessive HC formation (Fig. 2A′). Hyperplasticity was most
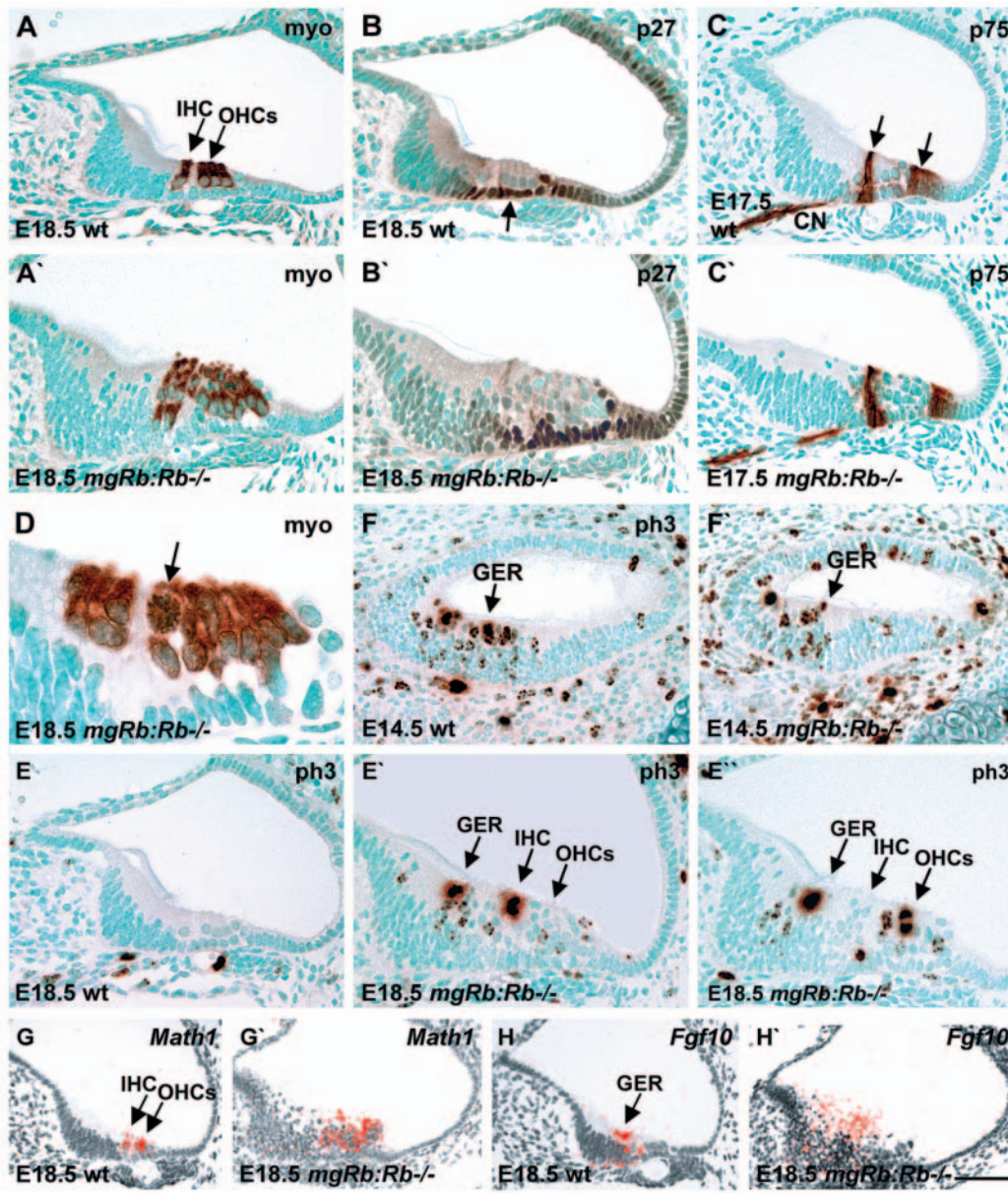
Development

Fig. 2. Proliferation and differentiation in the cochleas of *mgRb:Rb*$^{-/-}$ embryos. Myosin VI- and phospho-histone H3 immunostaining; *Math1* and *Fgf10* in situ hybridization. (A,A′) At birth, myosin VI is expressed in inner and outer HCs of control cochleas and also in supernumerary HCs of mutants. (B-C′) At late-embryogenesis, p27- and p75NTR-positive supporting cell populations (arrows) are seen both in controls and mutants. (D) A myosin VI-stained mitotic HC (arrow) in a mutant cochlea at birth. (E,E′) At birth, phospho-histone H3 staining shows ectopic mitoses in the greater epithelial ridge and the region of inner and outer HCs in mutant cochleas. These are not present in controls. (E″) Most of these mitotic HCs with strongly stained condensed chromatin are located near the lumen. (F,F′) At E14.5, phospho-histone H3-stained cells are seen in the caudal wall of the cochlea of both mutants and controls. (G,G′) At birth, *Math1* is expressed in cochlear HCs of controls and also in supernumerary HCs of mutants. (H,H′) At birth, *Fgf10* is expressed in the greater epithelial ridge of control cochleas and in the thickened ridge of mutants. Abbreviations: wt, wild type; ph3, phospho-histone H3; myo, myosin VI; GER, greater epithelial ridge; IHC, inner hair cell; OHCs, outer hair cells; CN, cochlear nerve. Scale bar: 70 μm for A-C′,E-F′); 30 μm for D; 80 μm for G-H′).

prominent in the basal half of the cochlea, where cellular differentiation is more advanced than in the apical half. When analysing transverse sections from the upper basal turn of E18.5 cochleas, myosin VI-positive area showed sixfold increase in the numbers of HC nuclei (*n*=6 mutant cochleas, mean±s.d. 23.2±4.3, contrasting with controls showing four HC nuclei in the same view). We first asked whether supernumerary HCs were generated at the expense of supporting cells. We used the CKI p27 (Fig. 2B,B′) and p75NTR (Fig. 2C,C′) as markers for differentiating supporting cells, the former one being expressed in the nuclei of several supporting cell populations, including pillar, Deiters', Hensen's and Claudius' cells, and the latter in the cytoplasm of pillar and Hensen's cells. p75NTR (Ngfr – Mouse Genome Informatics) was also expressed in the cochlear ganglion neurons. At E17.5 and E18.5, supporting cell numbers were not decreased in the mutants, rather, their numbers were increased, but not to the extent of HC overproduction. Based

on the analysis of transverse sections from the upper basal turn of E18.5 cochleas, a threefold increase in the numbers of p27-positive Deiters' plus pillar cells was found below HCs (*n*=6 mutant cochleas, mean±s.d. 14.5±3.1, contrasting with controls with five of these cells in a corresponding view).

Differentiating cochlear hair cells proliferate in the absence of *Rb*

A possible reason for the presence of supernumerary cochlear HCs in *mgRb:Rb*$^{-/-}$ mutants could be aberrant cell cycling. Perturbations in the activity of negative cell cycle regulators often lead to ectopic DNA synthesis, but manipulated cells can arrest at G2 and do not enter M phase (Novitch et al., 1996; Lipinski et al., 2001). To study the cell cycle status in the organ of Corti at E17.5 and E18.5, we used an M- and late G2-phase marker, phospho-histone H3. Although mitotic cells were not present in the control organ of Corti, prominent induction of mitoses was seen in the auditory sensory epithelium of

mgRb:Rb$^{-/-}$ mice (Fig. 2E-E″). The condensed chromatin of mitotic cells reacted strongly with the phospho-histone H3 antibody, while the G2-phase cells showed patchy staining of heterochromatin. *Rb* inactivation led to proliferation of differentiating HCs, as confirmed by the presence of mitotic figures in myosin VI-positive HCs (Fig. 2D). This was further confirmed by co-expression of phospho-histone H3 and calbindin, another marker for cochlear HCs (data not shown). Both inner (Fig. 2E′) and outer (Fig. 2E″) HCs were cycling in the mutants. Mitotic HCs showed a rounded morphology, characteristic of dividing cells (Fig. 2D). Most of them were found at the lumenal surface, but some also in deeper epithelial layers. Mitoses were not detected in the supporting cell layer. In addition to the organ of Corti, the greater epithelial ridge of the mutants showed prominent increase in thickness and high numbers of mitotic nuclei (Fig. 2E-E″), these results being in accordance with the observations of weak *Rb*/pRb expression in this ridge in normal animals (Fig. 1F). In conclusion, in contrast to controls where cells of the organ of Corti and almost all cells of the greater epithelial ridge are postmitotic at E18.5, *Rb* inactivation leads to ectopic cell cycles. Strikingly, differentiating HCs undergo mitoses in the *Rb*-deficient organ of Corti.

To determine the developmental time window of aberrant mitoses in the cochleas of *mgRb:Rb*$^{-/-}$ mutants, we next focused on earlier developmental stages. The bHLH gene *Math1* is one of the earliest markers for the HC lineage, being first expressed in the cochlea at E14.5 (Chen et al., 2002). This is followed by the induction of myosin VI at E15.5. At E13.5 (*n*=4 ears of mutants and controls each) and E14.5 (*n*=4 ears of mutants and controls each), the caudal wall of the cochlear duct, which houses precursor cells, showed comparable structure in *mgRb:Rb*$^{-/-}$ mutants and controls. At these stages, there was a slight increase in the numbers of phospho-histone 3-positive cells at the site of future organ of Corti in the mutants, but the increase was not statistically significant (Fig. 2F,F′, data not shown). By contrast, the adjacent mesenchyme of the mutants showed a clear increase in the amount of dividing cells, this being in line with the knowledge that *Rb* is expressed in the embryonic mesenchyme (Leezer et al., 2002). In the organ of Corti of the mutants, increased mitotic activity and overproduction of myosin VI-positive HCs became clear at E15.5 (*n*=8 ears of mutants and controls each), at the stage when pRb expression ensues in cochlear HCs of normal animals.

Available data show that in addition to a role as a repressor of cell cycle progression, depending on the cell context, *Rb* positively regulates differentiation by inducing expression of cell type-specific genes (Chen et al., 1996; Novitch et al., 1996; Novitch et al., 1999). To find out the possible role of *Rb* on cochlear HC differentiation, we studied the expression of a panel of early (*Math1*, myosins VI and VIIa, calbindin, *Fgf8*) and late (*Brn3c*) differentiation markers in *mgRb:Rb*$^{-/-}$ mutants at E17.5 and E18.5. *Math1* (Fig. 2G,G′) and the other markers (data not shown) were expressed in *Rb*-null cochlear HCs, similar to controls, although consistent with the expansion of HCs the signal covered a correspondingly wider zone. In normal animals, *Fgf8* is expressed in inner HCs, but not in outer HCs (Pirvola et al., 2002). Likewise, in the mutants, *Fgf8* expression was restricted to supernumerary inner HCs, indicating that cochlear HCs were subtyped despite their

overproduction (data not shown). Thus, despite the altered cytoarchitecture of the organ of Corti, cochlear HCs of the mutants showed a normal profile of molecules involved in differentiation and maturation.
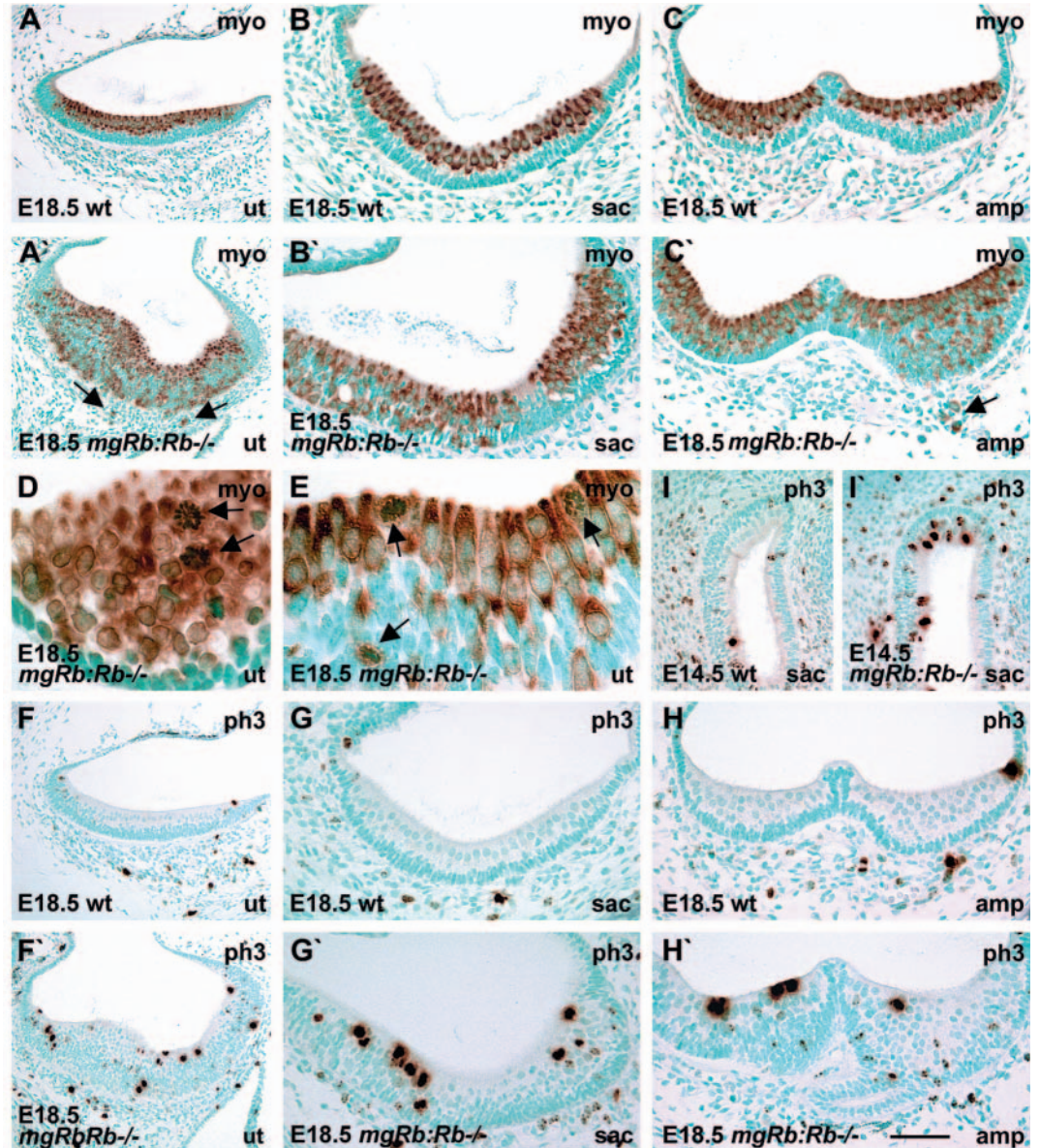
In addition, the greater epithelial ridge, the epithelial domain located medially to the organ of Corti, was hyperplastic in *mgRb:Rb*$^{-/-}$ mutants at birth (Fig. 2). Earlier studies have shown that *Fgf10* is expressed in the greater epithelial ridge (Pirvola et al., 2000; Pauley et al., 2003) (Fig. 2H) and this structure has been suggested to contain sensory precursor-like cells (Zheng and Gao, 2000; Woods et al., 2004). At birth, *Fgf10* was expressed throughout the abnormally thick greater epithelial ridge of the mutants, suggesting that ectopic cells in this region have characteristics of sensory precursor cells (Fig. 2H,H′).

Differentiating vestibular hair cells mitose in the absence of *Rb*

In addition to cochlear HCs, pRb was expressed in vestibular HCs (Fig. 1). We therefore studied the consequences of *Rb* loss in the vestibular sensory epithelia of *mgRb:Rb*$^{-/-}$ mice at E17.5 (*n*=8 ears) and E18.5 (*n*=15 ears). Prominent abnormalities were found (Fig. 3). Similar to the organ of Corti, *Rb* inactivation led to increase in the thickness of the vestibular sensory epithelia and to overproduction of myosin VI-positive HCs (Fig. 3A-C′). In normal sensory epithelia, HCs are situated lumenally and supporting cells basally. In the mutants, HCs were intermixed with supporting cells in the middle layers and the basal part of the epithelium was filled with supernumerary HCs. Moreover, some myosin VI-stained HCs were dislocated through the basal lamina into the mesenchyme (Fig. 3A′,C′). Mitotic figures were found in rounded, myosin VI-positive cells, demonstrating divisions of differentiating vestibular HCs (Fig. 3D,E), similar to *Rb*-null cochlear HCs (Fig. 2D). Most mitotic vestibular HCs were located at the lumenal surface, but some were seen at deeper epithelial levels (Fig. 3E) and in the mesenchyme. Accordingly, high numbers of phospho-histone H3-positive cells were observed in the vestibular sensory epithelia of the mutants, the majority of them at the lumenal surface, but some in deeper layers. By contrast, only a few dividing cells were found in control specimens (Fig. 3F-H′). Double-labelling experiments showed co-expression of phospho-histone H3 and calretinin, a marker for vestibular HCs, these data confirming that vestibular HCs of *mgRb:Rb*$^{-/-}$ mice undergo mitosis (data not shown). Similar to the situation at birth, at E14.5, high numbers of dividing HCs were found in the early-differentiating vestibular sensory epithelia of the mutants, in contrast to controls (*n*=6 ears of mutants and controls each) (Fig. 3I,I′).

Owing to differences in the timing of onset of differentiation, vestibular HCs at birth represent a more mature HC status when compared with cochlear HCs. Therefore, we also focused on the development of HC stereocilia in the vestibular organs. *Math1*, myosins VI and VIIa, calretinin, *Fgf8*, *Bdnf* and *Brn3c* were expressed in vestibular HCs of the mutants, similar to controls (data not shown). The fact that the neurotrophic factor *Bdnf* was expressed in supernumerary HCs suggests that these cells can attract neuronal endings for the establishment of synaptic contacts. Together, molecular differentiation of *Rb*-deficient vestibular HCs appears well advanced, similar to *Rb*-null auditory HCs. However, HCs of

Fig. 3. Mitosis and differentiation of vestibular hair cells of *mgRb:Rb^-/-* embryos. Myosin VI- and phospho-histone H3-immunostaining. (A,A') When compared with controls at birth, utricular sensory epithelia of mutants are hyperplastic because of an excess of myosinVI-positive HCs, some of which have penetrated into the mesenchyme (arrows). (B,B') In contrast to the saccular sensory epithelium of controls in which HCs occupy the lumenal layer, HCs are distributed throughout the epithelium in mutants. (C,C') In contrast to controls, ampullary sensory epithelia of mutants are hyperplastic because of overproduction of myosin VI-positive HCs, some of which invade the mesenchyme (arrow). (D) An oblique section through the utricular sensory epithelium of a mutant shows mitotic figures (arrows) in myosin VI-stained HCs. (E) A cross-section through the utricle shows that mitotic HCs (arrows) have rounded shape and occupy both lumenal and deeper epithelial layers. (F-H') Phospho-histone H3-stained utricular (F,F'), saccular (G,G') and ampullary (H,H') sensory epithelia at birth show higher numbers of mitotic cells in mutants when compared with controls. (I,I') At E14.5, early-differentiating saccular HCs of mutants undergo mitoses, in contrast to controls. Differentiating HCs occupy the lumenal layer and have a large nucleus. Abbreviations: wt, wild type; myo, myosin VI; ph3, phospho-histone H3. Scale bar: 120 μm for A,A',F,F'); 70 μm for B-C',G-I'; 30 μm for D,E.

the mutants showed abnormalities in the stereociliary bundle development, as evidenced by espin staining (Fig. 4A-H). Controls showed espin expression exclusively in stereocilia (Fig. 4A,E,G). In the mutants, espin-staining showed abnormal stereociliary bundle morphologies, particularly in utricles (Fig. 4B-F), but near-normal bundles were also seen, often in ampullae (Fig. 4G,H). Interestingly, supernumerary HCs in the deeper epithelial layers and in the mesenchyme showed espin-positive, disorganized cilia-like protusions and staining along cell membrane, indicating that the apicobasal polarity of these cells was lost (Fig. 4B-F).

Supernumerary hair cell production is partially compensated by apoptosis

In addition to the regulation of cell cycle progression and differentiation, several studies have shown that *Rb* inactivation

is associated with apoptosis. Because ectopic proliferation in the absence of *Rb* is rapidly balanced by massive apoptosis in many tissues, there are no obvious hyperplastic lesions (Zacksenhaus et al., 1996; Guo et al., 2001; Chen et al., 2004; MacPherson et al., 2004, Zhang et al., 2004). In contrast to other tissues, cleaved caspase 3- and TUNEL staining revealed apoptotic profiles only in part of sections through the mutant inner ear sensory epithelia at E17.5 and E18.5 (*n*=6 mutant ears at each stage). Myosin VI staining of nearby sections localized apoptosis to the regions of supernumerary cochlear (Fig. 5A-C) and vestibular HCs (Fig. 5D-F). Control sensory epithelia (*n*=6 ears at E18.5) showed very few apoptotic profiles (data not shown).

Rb loss can induce cell-autonomous apoptosis in certain tissues through the E2f1/p53/Apaf1 pathway (Morgenbesser et al., 1994; Macleod et al., 1996; Tsai et al., 1998; Jiang et al.,

Development

2000; Guo et al., 2001). To further evaluate the contribution of apoptosis to the mutant phenotype, we studied the compound $mgRb:Rb^{-/-}:Apaf1^{-/-}$ mutants (n=5 ears) and $mgRb:Rb^{-/-}:E2f1^{-/-}$ mutants (n=5 ears) at E18.5. The expectation was that Rb loss-induced apoptosis might be rescued to some extent by the concomitant $Apaf1$ or $E2f1$ inactivation and, thus, that the compound mutants might exhibit an increase in the amount of supernumerary HCs. The analysis revealed that, first, the morphology of the inner ear sensory epithelia of $Apaf1$ and $E2f1$ single null mutants was indistinguishable from controls and, second, the extent of HC overproduction in both types of compound mutants was comparable with $mgRb:Rb^{-/-}$ mutants (data not shown). Thus, apoptosis seems to be part of the altered phenotype, but does not prevent the distinct hyperplasia of Rb-deficient inner ear sensory epithelia at birth. The fact that we did not find deregulated cell cycle activity in these epithelia of $E2f1$-null mutants suggests that other E2f family members, which can bind pRb (E2f2, E2f3), regulate the expression of genes required for the G1- to S-phase progression either alone or redundantly with $E2f1$.

Rb loss induces hair cell multinucleation

To further study the developmental status of supernumerary HCs of $mgRb:Rb^{-/-}$ mutants at birth, we analysed 0.5 µm Toluidine Blue-stained plastic sections. Intermixture of HCs and supporting cells within the hyperplastic vestibular sensory epithelia was readily observed in the absence of Rb (Fig. 6A-H). In contrast to controls (Fig. 6A,G), the mutant sensory epithelia contained large numbers of HCs with a single, bizarre-shaped nucleus or with two (occasionally three or four) nuclei (Fig. 6B-E,H). Most of these HCs showed decondensed DNA. The occurrence of multinucleated HCs suggests that nuclear divisions had occurred without cytokinesis. Despite these distinct nuclear abnormalities, many of the lumenally located HCs showed near-normal stereociliary bundles (Fig. 6B,E,H). Many multinucleated HCs seemed to have a giant size, extending from the lumenal surface to the deeper epithelial strata (Fig. 6B,C,E). In addition to HCs with aberrant nuclear morphologies, small and rounded cells with mitotic figures in a single nucleus were seen, most of them at the epithelial surface (Fig. 6C-E,H). Many of these mitotic cells were identified as HCs, based on their immature stereociliary bundles and, in paraffin sections, on myosin VI expression (Fig. 3E). Thus, the hyperplastic phenotype of the inner ear sensory epithelia of $mgRb:Rb^{-/-}$ mutants seems to be caused by increase both in numbers and size of HCs. The relationship between the two types of Rb-null HCs is unclear, although in some cases HCs undergoing mitosis appeared to be derived
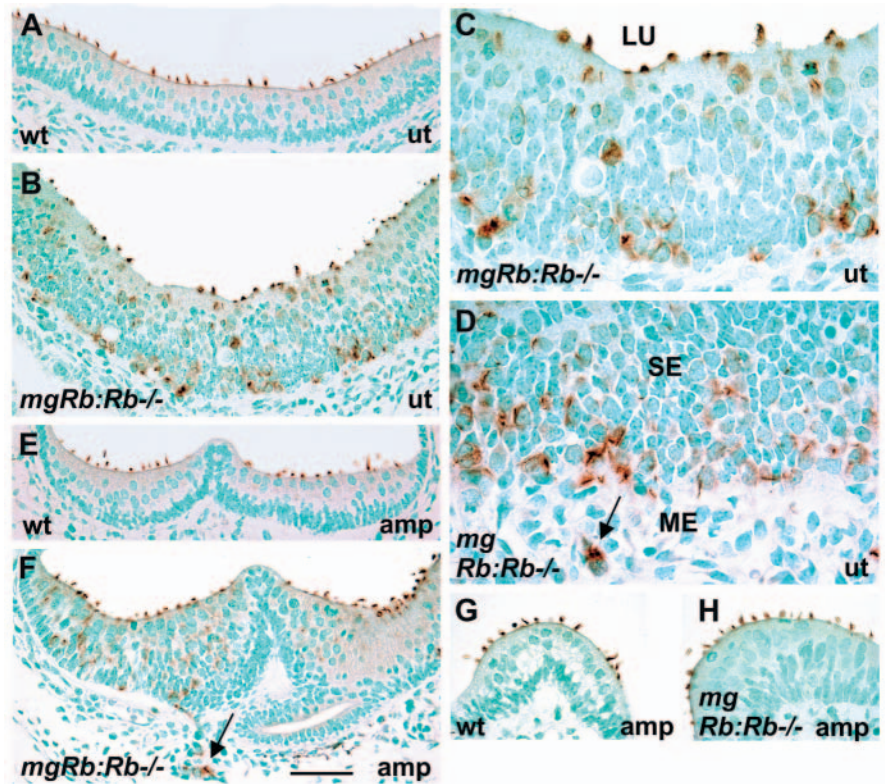

Fig. 4. Stereociliary bundles of vestibular hair cells of $mgRb:Rb^{-/-}$ mutants at birth, as shown by espin-immunostaining. (A) Espin is localized to HC stereocilia of control utricles. (B) In mutants, espin-positive HCs are situated throughout the thickened utricular sensory epithelium. Several HCs at the surface show abnormal bundles. (C,D) High magnification views show HCs with aberrant stereocilia in the utricle and in the adjacent mesenchyme (arrow) of mutants. (E,F) In contrast to controls, mutants show espin-stained HCs at different levels of the ampullary sensory epithelium. HCs in the mesenchyme are also espin positive (arrow). (G,H) In addition to the distinct bundle abnormalities, stereociliary bundle morphologies comparable with controls are seen in some HCs of mutants, especially in ampullae. Abbreviations: wt, wild type; ut, utricle; amp, ampulla; SE, sensory epithelium; ME, mesenchyme; LU, lumen. Scale bar: 70 µm for A-F; 60 µm for G,H; 30 µm for C,D.

from multinucleated HCs (data not shown). Based on observations made in some semi-thin sections, we cannot exclude the possibility that some supporting cells normally located basally in the sensory epithelia translocate to the lumenal surface and divide there (the mitotic cell marked with arrowhead in Fig. 6C). Consistent with an increase in apoptosis, as revealed by TUNEL- and cleaved caspase 3 staining (Fig. 5), semi-thin sections revealed scattered apoptotic profiles in the inner ear sensory epithelia of the mutants (Fig. 6D,F). The cytoplasm of some mitotic HCs exhibited signs of degeneration and, in a some cases, appeared apoptotic with condensed and fragmented nuclei (Fig. 6E,F). The organ of Corti of the mutants (Fig. 6I,J) showed similar pathological features to the vestibular sensory epithelia.

p21 is expressed in differentiating hair cells, but the null mutants have an unaltered inner ear phenotype

In our efforts to understand cell cycle regulation of HCs, we found that, in addition to Rb, the CKI $p21$ is expressed in developing vestibular and cochlear HCs (Fig. 7A-C). $p21$
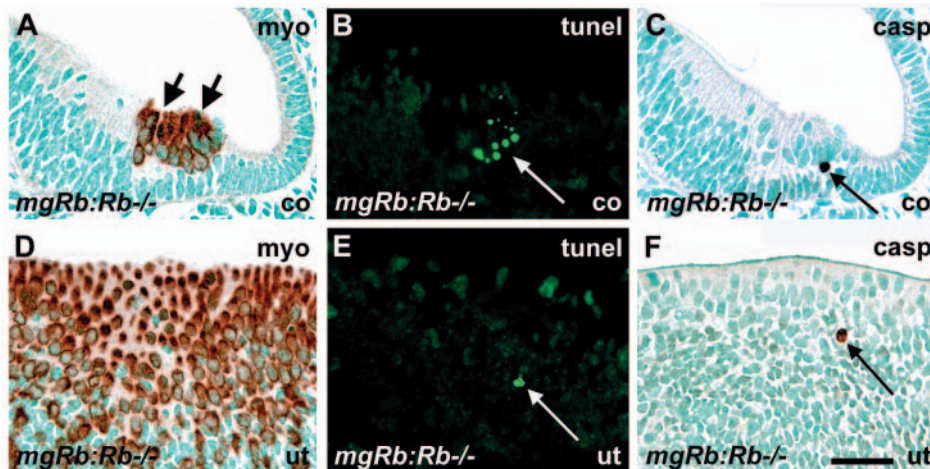
Fig. 5. Apoptosis in the inner ear of *mgRb:Rb*$^{-/-}$ mutants at E18.5. (A-C) In a mutant cochlea, the myosin VI-stained region of supernumerary HCs, which comprises mitotic figures (A, short arrows), shows TUNEL- (B) and cleaved caspase 3- (C) positive cells. Views are from adjacent sections. Compare with normal morphology in Fig. 2A. (D-F) TUNEL- and caspase 3-positive cells are present in the myosin VI-stained region of a hyperplastic utricular sensory epithelium. Compare with normal morphology in Fig. 3A. Long arrows indicate apoptotic profiles. Abbreviations: co, cochlea; ut, utricle; myo, myosin VI; casp, cleaved caspase 3. Scale bar: 60 μm.

expression was induced in vestibular HCs at E12.5 and in cochlear HCs at E14.5 (data not shown). By PN6, this expression was downregulated in vestibular HCs, while weak expression was still seen in cochlear HCs. Hair cells of the adult inner ear were devoid of *p21* (data not shown). Thus, in contrast to *Rb*, *p21* expression in HCs is restricted to developmental stages. In addition to HCs, *p21* was strongly expressed in some other structures of the developing inner ear: spiral limbus and stria vascularis of the cochlear duct; non-sensory epithelium of vestibular organs; endolymphatic duct; and the neurons of the cochlear and vestibular ganglia (Fig. 7A,C).

To address the role of p21 in the inner ear, we analysed the consequences of *p21* inactivation (Fig. 7D-H). Earlier studies have shown that *p21* knockout embryos develop into phenotypically normal adults (Deng et al., 1995), most likely owing to functional compensation between the CKI family members. However, previous studies have not specifically analysed *p21* null inner ears. At E16.5, E18.5, P2 and 2 months postnatally, we did not find morphological abnormalities in these mutant inner ears. Specifically, the cytoarchitecture of the vestibular and auditory sensory epithelia appeared normal (Fig. 7D-G) and there was no induction of proliferation (Fig. 7H). Taken together, the intriguing co-expression of *p21* and *Rb* in developing HCs suggests that p21 is an upstream regulator of pRb activity and that both cell cycle repressors account for the postmitotic state of developing HCs. The fact that *p21* knockouts exhibit a normal inner ear phenotype suggests redundancy between *p21* and another CKI(s).

Discussion

The present study shows that the *Rb* tumour suppressor gene and its encoded protein, pRb, are expressed in cochlear and vestibular HCs, both during the stages of differentiation and

during adulthood. We have dissected the requirement for *Rb* during HC development in *mgRb:Rb*$^{-/-}$ mutant mice, in which HCs are *Rb* negative. A main finding is the aberrant cycling of differentiating HCs. Differentiating and mature HCs are normally characterized by their permanent withdrawal from the cell cycle. Analysis of *mgRb:Rb*$^{-/-}$ mutants at birth, together with the expression data, suggest that pRb is required in a cell-autonomous manner for keeping differentiating HCs in a postmitotic state. As pRb expression was also detected in postnatal HCs, it is likely that its role as a negative cell cycle regulator is maintained during adulthood.

In several tissues, precursor cells permanently withdraw from the cell cycle before the onset of differentiation. This has also been shown to be the case in the embryonic cochlea (Chen et al., 2002). Although we could not see a clear effect of *Rb*-inactivation on the size of the precursor cell pool at E13.5 and E14.5, other observations suggest that pRb regulates the timing of their terminal mitoses. First, at these stages, there was a slight increase in the amount of phospho-histone 3-positive cells at the site of presumptive organ of Corti in *mgRb:Rb*$^{-/-}$ mice. Second, the greater epithelial ridge, which harbours precursor-like cells that can develop into HCs (Zhang et al., 2000; Woods et al., 2004), contained aberrantly cycling cells in the late-embryonic mutants. Third, in the cochleas of E18.5 mutants, the supporting cell population was to some extent expanded. As mitoses were not detected in the supporting cell layer of mutant cochleas, elevated numbers of precursor cells might contribute to this expansion. Based on our studies on the expression of members of the pocket protein family in the midgestational inner ear (U.P. and J.M., unpublished), the role of pRb on precursor cells appears to be to some extent redundant with other pocket proteins.

The present data show that HCs differentiate despite abnormal cell cycling, suggesting that HC proliferation and differentiation are uncoupled processes. Supernumerary HCs expressed a wide panel of markers characteristic for differentiating (and mature) HCs. During skeletal myogenesis, *Rb* stimulates the expression of differentiation markers by influencing *Myod1* activity (Gu et al., 1993; Novitch et al., 1996; Novitch et al., 1999; Zacksenhaus et al., 1996). A similar mechanism might occur in the developing inner ear, but as the interacting genes of the equivalent bHLH gene (*Math1*) in HCs have not been characterized, this possibility remains to be explored. *Rb*-null HCs at birth showed molecular evidence of differentiation, including expression of integral molecular constituents of stereocilia. However, supernumerary HCs situated in the deeper epithelial strata showed distinctly abnormal stereociliary bundles. At the lumenal surface, where stereociliary development normally occurs, large numbers of nascent bundles were seen. In many cases, this immaturity

Fig. 6. Mitosis, apoptosis and multinucleation of hair cells of *mgRb:Rb*$^{-/-}$ mutants at E18.5, as shown in semi-thin sections. (A) Normal utricular sensory epithelium shows HCs at the lumenal surface and underlying supporting cells. (B) A mutant utricle shows disorganized cell layering and HCs with an atypical nucleus or with two or more nuclei. Some of these HCs show near-normal stereociliary bundles. Some HCs seem to extend from the surface deep into the epithelium. (C) Mitotic cells with rounded morphology and nascent stereocilia (arrow) at the lumenal surface are intermixed with HCs with aberrant nuclear morphologies. A putative supporting cell that has translocated to the surface for mitosis is marked by an arrowhead. (D) Mitotic HCs (short arrows) are found mostly at the lumenal surface, but also in deeper layers, such as in this view where a cell undergoing mitosis is penetrating through the basal lamina. Scattered apoptotic profiles are also found (long arrows). (E,F) A mitotic cell (short arrow) showing signs of degeneration in the cytoplasm. Mitotic cells occasionally showed apoptotic figures (long arrow). (G,H) In contrast to controls, the ampullary sensory epithelia of mutants contain mitotic cells (arrows). In addition, several HCs with abnormal nuclei are found and many of them have stereociliary bundles with a morphology comparable with controls. (I,J) A transverse view through the organ of Corti of a normal cochlea shows four HCs and the underlying supporting cells. In the region of organ of Corti of mutants, high numbers of nuclei are seen, some of them having mitotic figures (short arrows) and a few apoptotic profiles (long arrow). Abbreviations: wt, wild type; ut, utricle; amp, ampulla; co, cochlea; LU, lumen, BL, basal lamina; ME, mesenchyme; HCs, hair cells; SCs, supporting cells; IHC, inner hair cell; OHCs, outer hair cells; P, pillar cell; Ds, Deiters' cell, H, Hensen's cell. Scale bar: 15 μm for A-J.
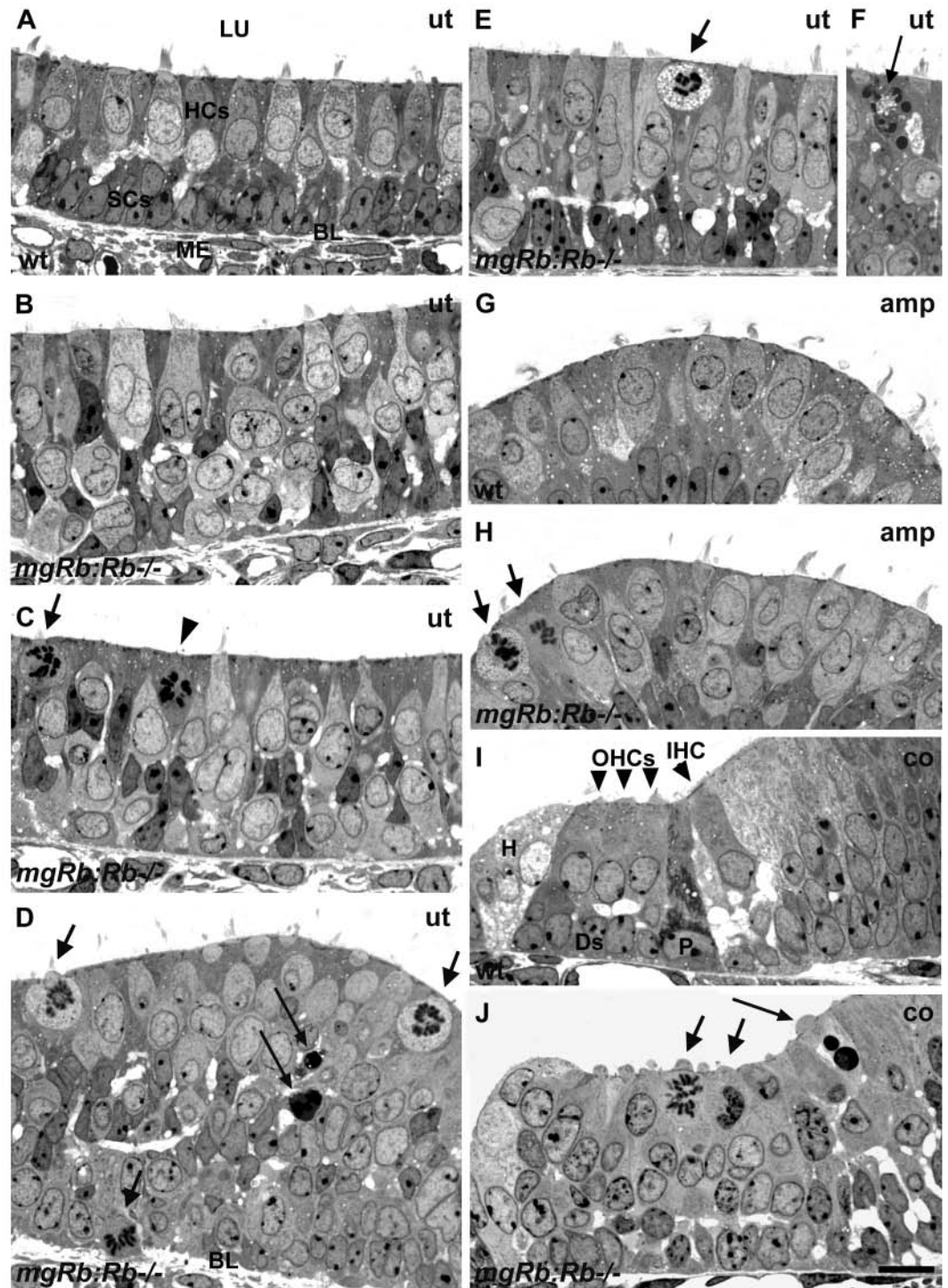
could be linked with HCs undergoing mitosis. Thus, the aberrant stereociliary development seems to be a consequence of deregulated cell cycles. The fact that stereociliary bundles of some of the supernumerary HCs appeared histologically almost comparable with controls implies they are functional in terms of mechanotransduction (Sage et al., 2005).

Using a phospho-histone H3 antibody, we were able to determine the kinetics of dividing HCs. Phospho-histone H3 is an M-phase marker, based on the fact that histone H3 Ser10 phosphorylation coincides with chromosome condensation of mitotic cells. Initiation of this phosphorylation is associated with heterochromatin of late G2 phase, and, thus, this antibody
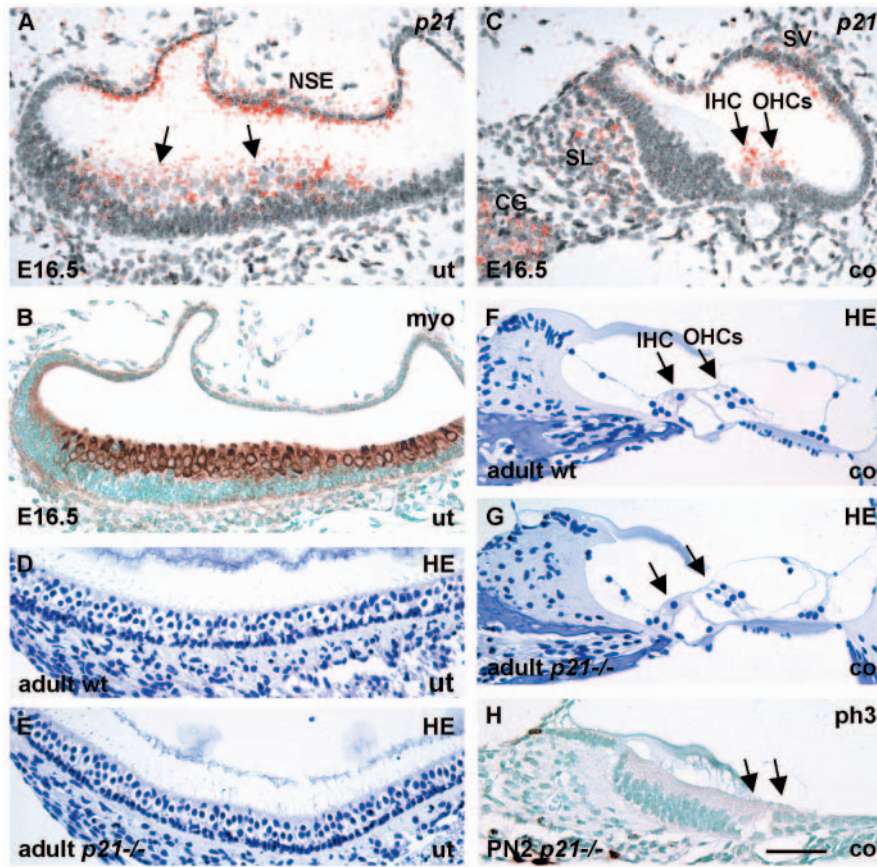
Fig. 7. *p21* expression in the developing inner ear and the phenotype of *p21* knockout mice. *p21* in situ hybridization; myosin VI and phospho-histone H3 immunostaining; Haematoxylin staining. (A,B) As shown in adjacent sections, *p21* and myosin VI are expressed in utricular HCs (arrows) at E16.5. *p21* is also found in the utricular non-sensory epithelium. (C) In the cochlea at E16.5, *p21* is expressed in HCs and in stria vascularis, spiral limbus and cochlear ganglion neurons. (D,E) Histology of the utricular sensory epithelium of adult *p21^{-/-}* mice is indistinguishable from controls, as shown by Haematoxylin staining. (F,G) Histology of the organ of Corti of adult *p21* knockouts is comparable with controls. (H) Mitoses are not induced in the cochleas of *p21*-null mutants, as shown at P2 by phospho-histone H3-staining (compare with control in Fig. 2E). Arrows in G,H indicate HCs. Abbreviations: wt, wild type; ut, utricle; co, cochlea; HE, Haematoxylin; SL, spiral limbus; CG, cochlear ganglion; SV, stria vascularis; IHC, inner hair cell; OHCs, outer hair cells; NSE, non-sensory epithelium; myo, myosin VI; ph3, phospho-histone H3. Scale bar: 70 μm for A-C,H; 80 μm for D-G.

seen deeper in the epithelia, indicating that translocation of nucleus or cell body to the surface is not a prerequisite for mitosis.

Our results suggest that postmitotic HCs retain the potential for cell cycle entry, but the pRb pathway acts as a guard to prohibit proliferation. The activity of pRb is probably kept in check by post-translational modifications, such as phosphorylation. Mitogens activate CDKs through upregulation of cyclins. A primary mechanism inhibiting CDK activity is the binding of CKIs to these kinases. CKIs efficiently inhibit CDKs even in the presence of cyclins (Olson et al., 2000). Indirect evidence for the importance of CDK regulation by CKIs in HCs comes from the fact that HCs do not proliferate in response to serum or mitogenic growth factors (Ryan, 2003).

Our data show that the CKI *p21* is expressed in the differentiating cochlear and vestibular HCs, and that the expression is induced at the initiation of HC differentiation. In the auditory sensory epithelium, *p21* expression was initiated at E14.5, at the stage when *Math1* expression has been first detected (Chen et al., 2002). It is possible that *p21* induction in HCs is regulated by *Math1*, in analogy to the positive role of bHLH proteins such as Myod1 and myogenin in skeletal myogenesis (Halevy et al., 1995; Guo et al., 1995). Thereafter, p21 together with other CKI(s) (see below) might have an active role in keeping pRb in a hypophosphorylated form. Thus, negative regulation at the level of both pRb and CKIs seems to be responsible for the maintenance of HC quiescence.

We did not find phenotypic alterations or aberrant mitoses in the inner ears of developing or adult *p21^{-/-}* mice (Fig. 7). Interestingly, in addition to *p21*, another CKI, *p19*, has been shown to be expressed in the late-embryonic organ of Corti, but its inactivation does not result in developmental abnormalities (Chen et al., 2003). Thus, functional redundancy may exist between *p21* and *p19* in developing cochlear HCs. In addition, developing vestibular HCs express *p21*, but do not show phenotypic changes following targeted gene disruption, most probably owing to functional compensation. The identity of the CKI that may cooperate with *p21* in vestibular HCs remains to be identified, as *p19* expression and the consequences of *p19* inactivation have not been reported in vestibular organs.

In contrast to developmental stages, we did not detect *p21* expression in adult HCs. Consistent with these observations are the data that cochlear HCs of *p19*-null mice show aberrant S-phase entry only during postnatal life (Chen et al., 2003). Interestingly, in the mature cochlea, *p19* inactivation was shown to have a stronger effect on inner HCs when compared with outer

is not completely M-phase specific (Hendzel et al., 1997; Van Hooser et al., 1998). The present results demonstrate, in controls and mutants, the difference between the strong staining of condensed chromatin of mitotic cells and the 'patchy' staining of heterochromatin of G2-phase cells. In the inner ear sensory epithelia of normal embryos, at the stages before HC differentiation, mitotic nuclei were invariably located to the lumenal surface. The majority of late G2-phase (this study) and S-phase cells (bromodeoxyuridine-positive) (e.g. Pirvola et al., 2002) are situated deeper in the sensory epithelia. This kind of relationship between nuclear position and the phase of cell cycle, termed as interkinetic nuclear migration, has been found in several types of developing epithelia, including the traumatized inner ear sensory epithelia of birds (Bhave et al., 1995). Also in *mgRb:Rb^{-/-}* mutants, most mitotic HCs were located to the epithelial surface. However, HCs undergoing mitosis were also

HCs (Chen et al., 2003), suggesting differences in the regulation of postmitotic state between the two cochlear HC subtypes. There might be differences in the expression of *p19* and/or other CKIs in these cells (postnatal expression of *p19* was not shown by Chen et al.) or cell cycle regulation downstream of CKIs might be different. The latter possibility is supported by the present data showing detectable expression of pRb in inner, but not outer, HCs of the adult cochlea. Interestingly, also in adult vestibular organs, pRb and *Rb* were expressed in a subset of HCs. Although non-labelled HCs may express pRb levels that are below the detection limit of the methods used, it remains to be determined whether this non-homogenous expression is linked to the morphological classification into type I and type II vestibular HCs (Wersäll and Bagger-Sjöbäck, 1974).

Existing data provide evidence for the sensitization of cells to apoptosis because of *Rb* loss-induced unscheduled proliferation at ectopic sites, although there is also evidence that pRb harbours inherent anti-apoptotic functions (Chau and Wang, 2003). We observed low-level apoptosis in the inner ear sensory epithelia of *mgRb:Rb⁻/⁻* mice at birth. The extent of this death did not compensate for the prominent hyperplasia of these epithelia, in marked contrast to several other *Rb*-deficient tissues showing massive cell-autonomous apoptosis in conjunction with ectopic proliferation (Zacksenhaus et al., 1996; Guo et al., 2001; Chen et al., 2004; MacPherson et al., 2004; Zhang et al., 2004). Thus, at least during development, the extent of apoptosis associated with *Rb* loss appears to be context dependent. The present data raise the issue of the fate of *Rb*-null HCs. Intriguingly, *Rb* loss induced HC cycling, but a large part of supernumerary HCs had defects in the completion of the cell cycle, with apparent failures in cytokinesis. The formation of multinucleated HCs, most of which appeared binucleated, implies for polyploidy. Based on the knowledge that polyploidy induced by manipulation of the cell cycle machinery often triggers cell death (Storchova and Pellman, 2004), the rate of apoptosis of supernumerary HCs may accelerate during postnatal life, an issue that can not be studied in the *mgRb:Rb⁻/⁻* mice because of their lethality at birth. The data that supernumerary HCs of adult *p19* knockout mice, which are generated postnatally rather than during embryogenesis, apoptose (Chen et al., 2003) support the possibility that *Rb*-deficient HCs may ultimately be lost. However, the aberrant proliferation, polyploidy and infiltration of *Rb*-null HCs into the mesenchyme may lead to neoplastic transformation.

In conclusion, the present work reveals unexpected plasticity of differentiating HCs. We show that the normally quiescent HCs proliferate in response to *Rb* loss and that these divisions are to a large extent tolerated, as analysed at birth. Continued *Rb* and pRb expression in mature HCs speaks for the role of this tumour suppressor as a guard against mitoses during adulthood as well. Our results point to the importance of upstream effectors of the CKI family in modulating pRb activity. While our work was under review, Sage et al. showed, in agreement with our results, that *Rb* inactivation induces HC proliferation (Sage et al., 2005). Similar to our data, they also showed that stereociliary bundles of *Rb*-null HCs were disoriented, but they also demonstrated that supernumerary HCs can function as mechanoelectric transducers. Our findings on the pathology of *Rb*-null HCs, including apoptosis, polyploidy and disorganization within and outside the inner ear sensory epithelia, were not reported by Sage et al. but suggest that HC quiescence is essential for the maintenance of coordinated development of these epithelia. Our

results suggest that forced HC proliferation may induce tumour cell-like and death-prone phenotypes. These data are likely to have implications in the design of future therapies to induce HC re-growth.

References

Bermingham, N. A., Hassan, B. A., Price, S. D., Vollrath, M. A., Ben-Arie, N., Eatock, R. A., Bellen, H. J., Lysakowski, A. and Zoghbi, H. Y. (1999). Math1: an essential gene for the generation of inner ear hair cells. *Science* **284**, 1837-1841.

Bhave, S. A., Stone, J. S., Rubel, E. W. and Coltrera, M. D. (1995). Cell cycle progression in gentamicin-damaged avian cochleas. *J. Neurosci.* **16**, 4618-4628.

Brugarolas, J., Chandrasekaran, C., Gordon, J. I., Beach, D., Jacks, T. and Hannon, G. J. (1995). Radiation-induced cell cycle arrest compromised by p21 deficiency. *Nature* **377**, 552-557.

Chau, B. N. and Wang, J. Y. (2003). Coordinated regulation of life and death by RB. *Nat. Rev. Cancer* **3**, 130-138.

Chen, P. L., Riley, D. J., Chen, Y. and Lee, W. H. (1996). Retinoblastoma protein positively regulates terminal adipocyte differentiation through direct interaction with C/EBPs. *Genes Dev.* **10**, 2794-2804.

Chen, P., Johnson, J. E., Zoghbi, H. Y. and Segil, N. (2002). The role of Math1 in inner ear development: Uncoupling the establishment of the sensory primordium from hair cell fate determination. *Development* **129**, 2495-2505.

Chen, P., Zindy, F., Abdala, C., Liu, F., Li, X., Roussel, M. F. and Segil, N. (2003). Progressive hearing loss in mice lacking the cyclin-dependent kinase inhibitor Ink4d. *Nat. Cell Biol.* **5**, 422-426.

Chen, D., Livne-bar, I., Vanderluit, J. L., Slack, R. S., Agochiya, M. and Bremner, R. (2004). Cell-specific effects of RB or RB/p107 loss on retinal development implicate an intrinsically death-resistant cell-of-origin in retinoblastoma. *Cancer Cell* **5**, 539-551.

Clarke, A. R., Maandag, E. R., van Roon, M., van der Lugt, N. M., van der Valk, M., Hooper, M. L., Berns, A. and te Riele, H. (1992). Requirement for a functional Rb-1 gene in murine development. *Nature* **359**, 328-330.

Classon, M. and Harlow, E. (2002). The retinoblastoma tumour suppressor in development and cancer. *Nat. Rev. Cancer* **2**, 910-917.

de Bruin A., Wu, L., Saavedra, H. I., Wilson, P., Yang, Y., Rosol, T. J., Weinstein, M., Robinson, M. L. and Leone, G. (2003). Rb function in extraembryonic lineages suppresses apoptosis in the CNS of Rb-deficient mice. *Proc. Natl. Acad. Sci. USA* **100**, 6546-6551.

Deng, C., Zhang, P., Harper, J. W., Elledge, S. J. and Leder, P. (1995). Mice lacking p21CIP1/WAF1 undergo normal development, but are defective in G1 checkpoint control. *Cell* **82**, 675-684.

Fekete, D. M., Muthukumar, S. and Karagogeos, D. (1998). Hair cells and supporting cells share a common progenitor in the avian inner ear. *J. Neurosci.* **18**, 7811-7821.

Ferguson, K. L., Vanderluit, J. L., Hebert, J. M., McIntosh, W. C., Tibbo, E., MacLaurin, J. G., Park, D. S., Wallace, V. A., Vooijs, M., McConnell, S. K. and Slack, R. S. (2002). Telencephalon-specific Rb knockouts reveal enhanced neurogenesis, survival and abnormal cortical development. *EMBO J.* **21**, 3337-3346.

Field, S. J., Tsai, F. Y., Kuo, F., Zubiaga, A. M., Kaelin, W. G. Jr, Livingston, D. M., Orkin, S. H. and Greenberg, M. E. (1996). E2F-1 functions in mice to promote apoptosis and suppress proliferation. *Cell* **85**, 549-561.

Fritzsch, B., Matei, V. A., Nichols, D. H., Bermingham, N., Jones, K., Beisel, K. W. and Wang, V. Y. (2005). Atoh1 null mutants show directed afferent fiber growth to undifferentiated ear sensory epithelia followed by incomplete fiber retention. *Dev. Dyn.* (in press).

Gu, W., Schneider, J. W., Condorelli, G., Kaushal, S., Mahdavi, V. and Nadal-Ginard, B. (1993). Interaction of myogenic factors and the

retinoblastoma protein mediates muscle cell commitment and differentiation. *Cell* **72**, 309-324.

Guo, K., Wang, J., Andres, V., Smith, R. C. and Walsh, K. (1995). MyoD-induced expression of p21 inhibits cyclin-dependent kinase activity upon myocyte terminal differentiation. *Mol. Cell. Biol.* **15**, 3823-3829.

Guo, Z., Yikang, S., Yoshida, H., Mak, T. W. and Zacksenhaus, E. (2001). Inactivation of the retinoblastoma tumor suppressor induces apoptosis protease-activating factor-1 dependent and independent apoptotic pathways during embryogenesis. *Cancer Res.* **61**, 8395-8400.

Halevy, O., Novitch, B. G., Spicer, D. B., Skapek, S. X., Rhee, J., Hannon, G. J., Beach, D. and Lassar, A. B. (1995). Correlation of terminal cell cycle arrest of skeletal muscle with induction of p21 by MyoD. *Science* **267**, 1018-1021.

Hasson, T., Gillespie, P. G., Garcia, J. A., MacDonald, R. B., Zhao, Y., Yee, A. G., Mooseker, M. S. and Corey, D. P. (1997). Unconventional myosins in inner-ear sensory epithelia. *J. Cell Biol.* **137**, 1287-1307.

Hendzel, M. J., Wei, Y., Mancini, M. A., Van Hooser, A., Ranalli, T., Brinkley, B. R., Bazett-Jones, D. P. and Allis, C. D. (1997). Mitosis-specific phosphorylation of histone H3 initiates primarily within pericentromeric heterochromatin during G2 and spreads in an ordered fashion coincident with mitotic chromosome condensation. *Chromosoma* **106**, 348-360.

Jacks, T., Fazeli, A., Schmitt, E. M., Bronson, R. T., Goodell, M. A. and Weinberg, R. A. (1992). Effects of an Rb mutation in the mouse. *Nature* **359**, 295-300.

Jiang, Z., Zacksenhaus, E., Gallie, B. L. and Phillips, R. A. (1997). The retinoblastoma gene family is differentially expressed during embryogenesis. *Oncogene* **14**, 1789-1797.

Jiang, Z., Liang, P., Leng, R., Guo, Z., Liu, Y., Liu, X., Bubnic, S., Keating, A., Murray, D., Goss, P. and Zacksenhaus, E. (2000). E2F1 and p53 are dispensable, whereas p21(Waf1/Cip1) cooperates with Rb to restrict endoreduplication and apoptosis during skeletal myogenesis. *Dev. Biol.* **227**, 8-41.

Jiang, Z., Guo, Z., Saad, F. A., Ellis, J. and Zacksenhaus, E. (2001). Retinoblastoma gene promoter directs transgene expression exclusively to the nervous system. *J. Biol. Chem.* **276**, 593-600.

Lee, E. Y., Chang, C. Y., Hu, N., Wang, Y. C., Lai, C. C., Herrup, K., Lee, W. H. and Bradley, A. (1992). Mice deficient for Rb are nonviable and show defects in neurogenesis and haematopoiesis. *Nature* **359**, 288-294.

Leezer, J. L., Hackmiller, R. C., Greene, R. M. and Pisano, M. M. (2002). Expression of the retinoblastoma family of tumor suppressors during murine embryonic orofacial development. *Orthod. Craniofacial Res.* **6**, 32-47.

Lipinski, M. M., Macleod, K. F., Williams, B. O., Mullaney, T. L., Crowley, D. and Jacks, T. (2001). Cell-autonomous and non-cell-autonomous functions of the Rb tumor suppressor in developing central nervous system. *EMBO J.* **20**, 3402-3413.

Liu, Y. and Zacksenhaus, E. (2000). E2F1 mediates ectopic proliferation and stage-specific p53-dependent apoptosis but not aberrant differentiation in the ocular lens of Rb deficient fetuses. *Oncogene* **19**, 6065-6073.

Macleod, K. F., Hu, Y. and Jacks, T. (1996). Loss of Rb activates both p53-dependent and independent cell death pathways in the developing mouse nervous system. *EMBO J.* **15**, 6178-6188.

MacPherson, D., Sage, J., Crowley, D., Trumpp, A., Bronson, R. T. and Jacks, T. (2003). Conditional mutation of Rb causes cell cycle defects without apoptosis in the central nervous system. *Mol. Cell. Biol.* **3**, 1044-1053.

MacPherson, D., Sage, J., Kim, T., Ho, D., McLaughlin, M. E. and Jacks, T. (2004). Cell type-specific effects of Rb deletion in the murine retina. *Genes Dev.* **18**, 1681-1694.

Morgenbesser, S. D., Williams, B. O., Jacks, T. and DePinho, R. A. (1994). p53-dependent apoptosis produced by Rb-deficiency in the developing mouse lens. *Nature* **371**, 72-74.

Murray, A. W. (2004). Recycling the cell cycle: cyclins revisited. *Cell* **116**, 221-234.

Novitch, B. G., Mulligan, G. J., Jacks, T. and Lassar, A. B. (1996). Skeletal muscle cells lacking the retinoblastoma protein display defects in muscle gene expression and accumulate in S and G2 phases of the cell cycle. *J. Cell Biol.* **135**, 441-456.

Novitch, B. G., Spicer, D. B., Kim, P. S., Cheung, W. L. and Lassar, A. B. (1999). pRb is required for MEF2-dependent gene expression as well as cell-cycle arrest during skeletal muscle differentiation. *Curr. Biol.* **9**, 449-459.

Olson, N. E., Kozlowski, J. and Reidy, M. A. (2000). Proliferation of intimal smooth muscle cells. Attenuation of basic fibroblast growth factor 2-stimulated proliferation is associated with increased expression of cell cycle inhibitors. *J. Biol. Chem.* **275**, 11270-11277.

Pauley, S., Beisel, K., Wright, T., Pirvola, U., Ornitz, D. and Fritzsch, B.

(2003). Expression and function of FGF10 in mammalian inner ear development. *Dev. Dyn.* **227**, 203-215.

Pirvola, U., Spencer-Dene, B., Xing-Qun, L., Kettunen, P., Thesleff, I., Fritzsch, B., Dickson, C. and Ylikoski, J. (2000). FGF/FGFR-2(IIIb) signaling is essential for inner ear morphogenesis. *J. Neurosci.* **20**, 6125-6134.

Pirvola, U., Ylikoski, J., Trokovic, R., Hebert, J. M., McConnell, S. K. and Partanen, J. (2002). FGFR1 is required for the development of the auditory sensory epithelium. *Neuron* **35**, 671-680.

Pirvola, U., Zhang, X., Mantela, J., Ornitz, D. M. and Ylikoski, J. (2004). Fgf9 signaling regulates inner ear morphogenesis through epithelial-mesenchymal interactions. *Dev. Biol.* **273**, 350-360.

Ryan, A. F. (2003). The cell cycle and the development and regeneration of hair cells. *Curr. Top. Dev. Biol.* **57**, 449-466.

Ruben, R. J. (1967). Development of the inner ear of the mouse: a radioautographic study of terminal mitoses. *Acta Otolaryngol. Suppl.* **220**, 1-44.

Sage, C., Huang, M., Karimi, K., Gutierrez, G., Vollrath, M. A., Zhang, D. S., Garcia-Anoveros, J., Hinds, P. W., Corwin, J. T., Corey, D. P. and Chen, Z. Y. (2005). Proliferation of functional hair cells in vivo in the absence of the retinoblastoma protein. *Science* **307**, 1114-1118.

Sellers, W. R., Novitch, B. G., Miyake, S., Heith, A., Otterson, G. A., Kaye, F. J., Lassar, A. B. and Kaelin, W. G. Jr (1998). Stable binding to E2F is not required for the retinoblastoma protein to activate transcription, promote differentiation, and suppress tumor cell growth. *Genes Dev.* **12**, 95-106.

Storchova, Z. and Pellman, D. (2004). From polyploidy to aneuploidy, genome instability and cancer. *Nature Rev.* **5**, 45-54.

Takahashi, C., Bronson, R. T., Socolovsky, M., Contreras, B., Lee, K. Y., Jacks, T., Noda, M., Kucherlapati, R. and Ewen, M. E. (2003). Rb and N-ras function together to control differentiation in the mouse. *Mol. Cell. Biol.* **23**, 5256-5268.

Tsai, K. Y., Hu, Y., Macleod, K. F., Crowley, D., Yamasaki, L. and Jacks, T. (1998). Mutation of E2f-1 suppresses apoptosis and inappropriate S phase entry and extends survival of Rb-deficient mouse embryos. *Mol. Cell* **3**, 293-304.

Van Hooser, A., Goodrich, D. W., Allis, C. D., Brinkley, B. R. and Mancini, M. A. (1998). Histone H3 phosphorylation is required for the initiation, but not maintenance, of mammalian chromosome condensation. *J. Cell Sci.* **111**, 3497-3506.

Vidal, A. and Koff, A. (2000). Cell-cycle inhibitors: three families united by a common cause. *Gene* **247**, 1-15.

Weinberg, R. A. (1995). The retinoblastoma protein and cell cycle control. *Cell* **81**, 323-330.

Wersäll, J. and Bagger-Sjöbäck, D. (1974). Morphology of the vestibular sense organ. In: *Handbook of Sensory Physiology. Vestibular System. Basic Mechanisms* (ed. H. H. Kornhuber), pp. 123-170. New York: Springer.

Wilkinson, D. G and Green, J. (1991). In situ hybridization and the three-dimensional construction of serial sections. In: *Postimplantation Mammalian Embryos* (ed.. A. J. Copp and D. L. Cockroft), pp. 155-171. Oxford, UK: IRL Press.

Woods, C., Montcouquiol, M. and Kelley M. W. (2004). Math1 regulates development of the sensory epithelium in the mammalian cochlea. *Nat. Neurosci.* **7**, 1310-1318.

Wu, L., de Bruin, A., Saavedra, H. I., Starovic, M., Trimboli, A., Yang, Y., Opavska, J., Wilson, P., Thompson, J. C., Ostrowski, M. C. et al. (2003). Extra-embryonic function of Rb is essential for embryonic development and viability. *Nature* **421**, 942-947.

Yoshida, H., Kong, Y. Y., Yoshida, R., Elia, A. J., Hakem, A., Hakem, R., Penninger, J. M. and Mak, T. W. (1998). Apaf1 is required for mitochondrial pathways of apoptosis and brain development. *Cell* **94**, 739-750.

Zacksenhaus, E., Jiang, Z., Chung, D., Marth, J. D., Phillips, R. A. and Gallie, B. L. (1996). pRb controls proliferation, differentiation, and death of skeletal muscle cells and other lineages during embryogenesis. *Genes Dev.* **10**, 3051-3064.

Zhang, J., Gray, J., Wu, L., Leone, G., Rowan, S., Cepko, C. L., Zhu, X., Craft, C. M. and Dyer, M. A. (2004). Rb regulates proliferation and rod photoreceptor development in the mouse retina. *Nat. Genet.* **36**, 351-360.

Zheng, J. L. and Gao, W. O. (2000). Overexpression of Math1 induces robust production of extra hair cells in postnatal rat inner ears. *Nat. Neurosci.* **3**, 580-586.

Zheng, L., Sekerkova, G., Vranich, K., Tilney, L. G., Mugnaini, E. and Bartles, J. R. (2000). The deaf jerker mouse has a mutation in the gene encoding the espin actin-bundling proteins of hair cell stereocilia and lacks espins. *Cell* **102**, 377-385.